Journal of Engineering and Applied Sciences 14 (Special Issue 8): 10406-10412, 2019
ISSN: 1816-949X

Coupled-Channel Calculations for Fusion Cross Section and Fusion Barrier Distribution of $^{32}S+^{144, 150, 152, 154}Sm$

[1,3]Adil J. Najim, [2]Fouad A. Majeed and [1]Khalid H. H. Al-Attiyah
[1]Department of Physics, College of Sciences,
[2]Department of Physics, College of Education for Pure Sciences,
University of Babylon, Babylon, Iraq
[3]Department of Physics, College of Education for Pure Sciences,
University of Kerbala, Karbala, Iraq

Abstract: In this research, the fusion cross section σ_{fus} and fusion barrier distribution D_{fus} have been investigated below and above the Coulomb barrier using coupled-channel method with CCFULL Fortran code for $^{32}S+^{144,150,152,154}Sm$ reactions and compare the calculated properties with experimental data. The deformation parameters of projectile and target nuclei have been taken into account for all reactions.The first and second reactions $^{32}S+^{144,150}Sm$, the vibrational coupling has been considered for both projectile and target nuclei while for the third and fourth reactions $^{32}S+^{152,154}Sm$, the coupling of rotational levels for target nucleus have been taken and the vibrational coupling remain the same for the projectile. The results show that the coupling calculations of fusion cross sectionhave shown an enhancement with respect to the experimental data, especially, for $^{32}S+^{152,154}Sm$ reactions, consequently, the calculated fusion barrier distribution agreed reasonably well with extracted fusion barrier distribution.

Key words: Fusion cross section, fusion barrier distribution, heavy-ion fusion, coupled-channel method, experimental data, fusion barrier

INTRODUCTION

The fusion cross section in interest represents the probability of fusion of two separated nuclei to form a compound nucleus as a result of overcoming on the Coulomb barrier which formed as a consequence of the strong cancellation between nuclear and Coulomb forces. In some circumstances, it is possible to assume that the fused nuclei are structure less, i.e., neglecting the internal degrees of freedom. This approach is called the one dimensional potential model which represents the potential as a function of one variable called the relative distance (r). This model gives good predictions for light systems while for heavy systems the calculated fusion cross section becomes underestimation in the region below the Coulomb barrier then the coupling to the internal degrees of freedom becomes unavoidable. When the colliding nuclei come close together they may be excited to low lying excited states or a nucleons transfer process could appear, all that could take place before the compound nucleus to be form. In this situation, the elastic channel couples with non-elastic channels and the transmission process through the barrier occur in each channel where all these transmission probabilities must be account to obtain the total transmission into the barrier (Frobrich and Lipperheide, 1996; Dasgupta *et al*., 1998; Hagino and Takigawa, 2012).

In heavy-ion fusion reactions around the Coulomb barrier, the effect of tunneling phenomena becomes more remarkable, specifically at low incident energy, i.e., below the Coulomb barrier or in the region called the classically for bidden region (Dasgupta *et al*., 1998; Balantekin and Takigawa, 1998). The best current method to manipulate the couplings between radial distance and internal degrees of freedom of colliding nuclei is the numerical solution of coupled channel equations. This coupling is represented by taken into account the static rotational deformations, vibrational modes or nucleons transfer processes and it is represented by the distribution of fusion barriers (Dasgupta *et al*., 1998; Hagino and Takigawa, 2012; Dasso *et al*., 1983a, b; Nagarajan *et al*., 1986; Esbensen, 1981).

The importance of fusion barrier distribution makes it a focus of interesting for many researchers (Najim *et al*., 2019; Canto and Donangelo, 2009; Hagino, 2016) where its shape gives significant information on the reaction dynamics as well as structures of colliding nuclei (Majeed *et al*., 2017; 2019).

MATERIALS AND METHODS

Theoretical background

Coupled-channel formalism: The coupled-channel method treats the collision between two nuclei by

Corresponding Author: Adil J. Najim, Department of Physics, College of Sciences, University of Babylon, Babylon, Iraq

coupling the relative motion variable $r=(r,\hat{r})$ with variable of intrinsic motion ξ, the Hamiltonian of coupled channel is given by Frobrich and Lipperheide (1996), Hagino and Takigawa (2012) and Hagino *et al.* (1999):

$$H(r,\xi)=-\frac{\hbar^2}{2\mu}\nabla^2+V_0(r)+h_0(\xi)+V_{coup}(r,\xi) \quad (1)$$

Where:

$h(\xi)$ and V_{coup} : The internal and coupling Hamiltonians, respectively

$V_0(r)$: The potential of relative motion and is given by:

$$V_0(r)=V_0^N(r)+V_0^C(r)=-\frac{V_0}{1+\exp((r-R_0)}+\frac{Z_pZ_Te^2}{r} \quad (2)$$

Where:

$V_0^N(r)$: The nuclear part given by Woods-Saxon potential

$V_0^C(r)$: The Coulomb part

$V_{coup}(r,\xi)$ can be expanded as multipoles:

$$V_{coup}(r,\xi)=\sum_{\lambda>0}f_\lambda(r)Y_\lambda(\hat{r}).T_\lambda(\xi) \quad (3)$$

Where:

$(Y_\lambda(\hat{r}).T_\lambda(\xi))$: The scalar product of spherical harmonic

$Y_\lambda(\hat{r})$: Spherical tensor $T_\lambda(\xi)$

The channel wavefunctions can be defined as the expansion of intrinsic wave functions $\varphi_{\alpha I m_I}(\xi)$:

$$\langle\hat{r}\xi|(\alpha lI)JM\rangle=\sum_{m_l,m_I}\langle lm_l\,Im_I|JM\rangle Y_{lm_l}(\hat{r})\varphi_{\alpha Im_I}(\xi) \quad (4)$$

Where:

J : The total angular momentum

M : Its z component

l and I : The orbital and intrinsic angular momenta, respectively

The intrinsic wave functions $\varphi_{\alpha Im_I}(\xi)$ satisfy the Schrodinger equation in terms of intrinsic Hamiltonian with $\in_{\alpha I}$ eigenvalues:

$$h_0(\xi)\varphi_{\alpha Im_I}(\xi)=\in_{\alpha I}\varphi_{\alpha Im_I}(\xi) \quad (5)$$

where, α denotes other quantum numbers except I. The total wave function can be represented as expansion of the channel wave functions:

$$\Psi_J(r,\xi)=\sum_{\alpha,l,I}\frac{u^J_{\alpha lI}(r)}{r}\langle\hat{r}\xi|(\alpha lI)JM\rangle \quad (6)$$

For the $u^J_{\alpha lI}(r)$ wave functions, the coupled-channel equations are:

$$\left[-\frac{\hbar^2}{2\mu}\frac{d^2}{dr^2}+\frac{l(l+1)\hbar^2}{2\mu r^2}+V_0(r)+\in_{\alpha I}-E\right]u^J_{\alpha lI}(r)=\sum_{\alpha',l',I'}V^J_{\alpha lI,\alpha',l',I'}(r)u^J_{\alpha',l',I'}(r) \quad (7)$$

where, $V^J_{\alpha lI,\alpha',l',I'}(r)$ are the coupling matrix elements given by:

$$V^J_{\alpha lI,\alpha',l',I'}(r)=\langle(\alpha lI)JM|V_{coup}(r,\xi)|(\alpha',l',I')JM\rangle=\sum_\lambda(-1)^{I-I'+l'+J}f_\lambda(r)\langle l'||Y_\lambda||l'\rangle\langle\alpha lI||T_\lambda||\alpha'I'\rangle \quad (8)$$

$$\times\sqrt{(2l+1)(2I+1)}\begin{Bmatrix} I' & l' & J\\ l & I & \lambda\end{Bmatrix} \quad (9)$$

With no-Coriolis approximation, the relative angular momentum for each channel can be replaced with total angular momentum J (Hagino and Takigawa, 2012; Hagino *et al.*, 1999) and for more simplicity, we denote n for (αlI). Then, Eq. 7 is solved with incoming wave boundary conditions which are:

$$u_n(r)=\begin{cases} T_n\exp\left(-i\int_{r_{abs}}^{r}k_n(r')dr'\right) & \text{for } r\le r_{min}\\ H_J^{(-)}(k_nr)\delta_{n,n_i}-R_nH_J^{(+)}(k_nr) & \text{for } r\to\infty\end{cases} \quad (10)$$

Where:

$$k_n(r)=\sqrt{\frac{2\mu}{\hbar^2}\left(E-\in_n-\frac{J(J+1)\hbar^2}{2\mu r^2}-V_N(r)-\frac{Z_pZ_Te^2}{r}-V_{nn}(r)\right)} \quad (11)$$

where, $k_n(r)$ is the local wave-number for the nth channel and (Hagino and Takigawa, 2012; Hagino *et al.*, 1999). Once, the transmission coefficient T_n is calculated then the penetrability $P_J(E)$ is:

$$P_J(E)=\sum_n\frac{k_n(r_{min})}{k_0}|T_n|^2 \quad (12)$$

Finally, the fusion cross section is given by:

$$\sigma_{fus}(E)=\frac{\pi}{k_0^2}\sum_J(2J+1)P_J(E) \quad (13)$$

The coupled-channels method with no-Coriolis approximation is programmed by Hagino *et al.* (1999) it takes into account the effects of nonlinear coupling to all orders. This code is abbreviated as CCFULL code.

Fusion barrier distribution: The fusion barrier distribution has been extracted from experimental data, the definition supposed by Rowley *et al.* (1991) has been adopted:

$$D_f(E)=\frac{d^2(E\sigma)}{dE^2} \quad (14)$$

Where:
E : The center of mass energy
σ : Fusion cross section

Numerically, the point difference method was used to calculate D_f (E) (Dasgupta *et al.*, 1998) for both the experimental and calculated cross sections:

$$\frac{d^2(E\sigma)}{dE^2}=2\left[\frac{(E\sigma)_3-(E\sigma)_2}{E_3-E_2}-\frac{(E\sigma)_2-(E\sigma)_1}{E_2-E_1}\right]\left(\frac{1}{E_3-E_1}\right) \quad (15)$$

And for equally spaced data the Eq. 15 becomes:

$$\frac{d^2(E\sigma)}{dE^2}=\left(\frac{(E\sigma)_3-2(E\sigma)_2+(E\sigma)_1}{\Delta E^2}\right) \quad (16)$$

Calculated at Energy E:

$$E=\frac{E_1+2E_2+E_3}{4} \quad (17)$$

With statistical error defined as:

$$\delta_c\approx\left(\frac{E}{\Delta E^2}\right)\left[(\delta\sigma)_1^2+4(\delta\sigma)_2^2+(\delta\sigma)_3^2\right]^{1/2} \quad (18)$$

where, δσ is the statistical error in fusion cross section. Another method was used to calculate fusion barrier distribution depending on the least square fitting of Wong's formula with experimental data (Najim *et al.*, 2019) where the second derivative of Eσ is:

$$\frac{d^2(E\sigma)}{dE^2}=\frac{2\pi^2R_b^2}{\hbar\omega}\frac{\exp(x)}{(1+\exp(x))^2} \quad (19)$$

Where:
x : $2\pi(E-V_b)/\hbar\omega$
V_b : The fusion barrier height
ħω : The curvature

Table 1: Potential parameters

System	V_0 (MeV)	r_0 (fm)	a_0 (fm)	V_b (MeV)	R_b (fm)
$^{32}S+^{144}Sm$	150	0.99	0.70	130.37	10.15
$^{32}S+^{150}Sm$	150	1.01	0.62	130.01	10.29
$^{32}S+^{152}Sm$	145	1.00	0.76	126.24	10.43
$^{32}S+^{154}Sm$	160	0.99	0.70	128.12	10.35

RESULTS AND DISCUSSION

The four systems had been investigated by using CCFULL Fortran code with two different modes of excitation both in the projectile and in the target. This code uses Woods-Saxon potential, the parameters of this potential were adjusted in order to get best fits to fusion cross section for the systems under investigation these parameters are displayed in Table 1. Table 2 and 3 display the adopted deformation parameters and excited levels in the calculations for each nucleus.

To extract the fusion barrier distribution from experimental data, Eq. 15 had been carried out with energy interval ΔE greater or equals to 2 MeV and Eq. 16 for the calculated fusion barrier with E equals 2 MeV. The detailed results for the systems under study are shown below:

$^{32}S+^{144}Sm$ system: Figure 1a shows the fusion cross section of $^{32}S+^{144}Sm$ system calculated by the CCFULL code. The coupling cross section is taken as the projectile and target have vibrational modes where the low-lying levels of ^{32}S which have been coupled are 2^+ and 3^- and that of ^{144}Sm are also 2^+ and 3^-. The best value of fusion barrier had been gotten for this system that reproduced the experimental data is 130.37 MeV and the best collection of Woods-Saxon parameters for this barrier is listed in Table 1 where we try to get a best value of potential height V_0 to avoid as much as possible the oscillation in the fusion barrier distribution in the same time the diffuseness parameter a_0 that gives the best approach with experimental data must be not small, so, its value was 0.70. The experimental fusion cross section had been taken from reference (Glagola *et al.*, 1984). We note the great enhancement of calculated cross section using coupling to low-lying excited states (solid line) in compare with no-coupling (dash line). However, the calculated cross sections are under estimated at lower energies.

Figure 1b shows the calculated fusion barrier distribution for coupling (solid line), no-coupling (dashed line), extracted fusion barrier distribution using point difference formula (black circle) and the calculated using Wong's formula (red circle) (Najim *et al.*, 2019). The statistical errors of extracted fusion barrier distribution using point difference formula have been removed because they are so, large compare with other curves. We note that almost both the coupling curve and point difference formula approach each other in good manner,

Table 2: Parameters of vibrational calculations

Nucleus	Radius parameter	λ^{π}	E^{*}(MeV)	β_{λ}
^{32}S	1.16	2_1^+	2.2306 Prytychenko *et al*. (2016)	0.308 Prytychenko *et al*. (2016)
		3_1^-	5.006 Kibedi and Spear (2002)	0.534 Kibedi and Spear (2002)
^{144}Sm	1.06	3_1^-	1.810 Leigh *et al*. (1995)	0.205 Leigh *et al*. (1995)
		2_1^+	1.660 Leigh *et al*. (1995)	0.110 Leigh *et al*. (1995)
^{150}Sm	1.06	3_1^-	1.071 Kibedi and Spear (2002)	0.145 Kibedi and Spear (2002)
		2_1^+	0.334 Prytychenko *et al*. (2016)	0.193 Prytychenko *et al*. (2016)

Table 3: Parameters of rotational calculations

Nucleus	Radius parameter	E^{*} (MeV) Raghavan (1989)	β_2	β_4	No. of levels
^{152}Sm	1.06	0.1218	0.237	0.097	4
^{154}Sm	1.06	0.0820	0.270	0.105	4

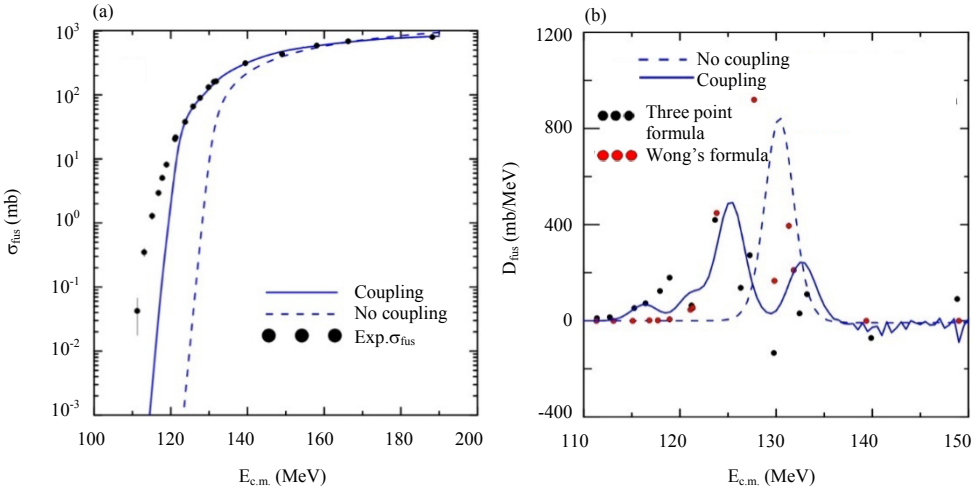

Fig. 1: (a) The experimental fusion cross section for ^{32}S+^{144}Sm along with results from CC calculations using CCFULL and (b) The fusion barrier distribution for the same system

although, they are not identical while the calculated fusion barrier distribution using Wong's formula has shown two peaks with a height relativity large than other curves.

^{32}S+^{150}Sm system: Figure 2a shows the fusion cross section of ^{32}S+^{150}Sm system calculated by the CCFULL code. As the previous system, the vibrational coupling with single phonon is taken for both the projectile and target where the same low-lying levels of ^{32}S had been coupled which are 2^+ and 3^- and that of ^{150}Sm are also 2^+ and 3^-. The fusion barrier V_b is 130.01 MeV with Radius R_b equals 10.29 fm. The Woods-Saxon parameters are V_0 = 150 MeV, r_0 = 1.01 fm and a = 0.62 fm. The experimental fusion cross section (black circles) had been taken from reference (Glagola *et al*., 1984). The good enhancement of calculated cross section using coupling (solid line) is clear in comparing with the no-coupling (dash line). However, the coupling cross section reproduced the experimental data very well in the range above about 120 MeV, nevertheless it is underestimated in the range of lower energies.

Figure 2b shows the calculated fusion barrier distribution for coupling (solid line), no-coupling (dashed line), extracted fusion barrier distribution using point difference formula (black circle) and the calculated using Wong's formula (red circle) (Najim *et al*., 2019). We note that the coupling curve almost takes the same behavior as the extracted fusion barrier distribution but with little difference, so, it can be concluded that the fusion process for this system is greatly affected by the excitation to the low-lying levels for both the projectile and the target. However, the difference between them may be attributed to other types of coupling or to high intense vibrational modes which could not be taken into account.

^{32}S+^{152}Sm system: Figure 3a shows the results of the calculated fusion cross section for ^{32}S+^{152}Sm system where the coupling curve (solid line) taken to the rotational levels of ^{152}Sm nucleus along with vibrational modes of ^{32}S which are illustrated in Table 2 and 3, the no-coupling curve is represented by (dash line) and the experimental data (black circle) has been taken from reference (Glagola *et al*., 1984). It is clear from this figure

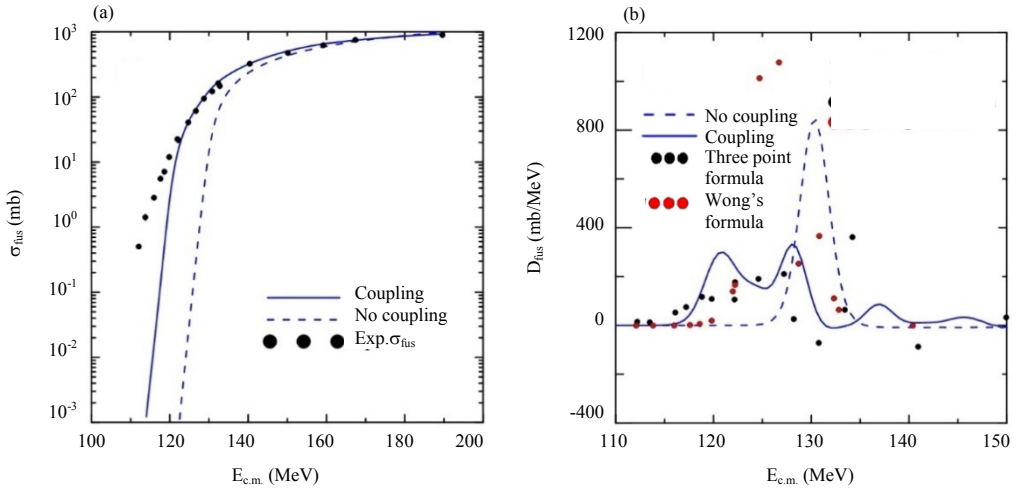

Fig. 2: (a) The experimental fusion cross section for $^{32}S+^{150}Sm$ along with results from CC calculations using CCFULL and (b) The fusion barrier distribution for the same system

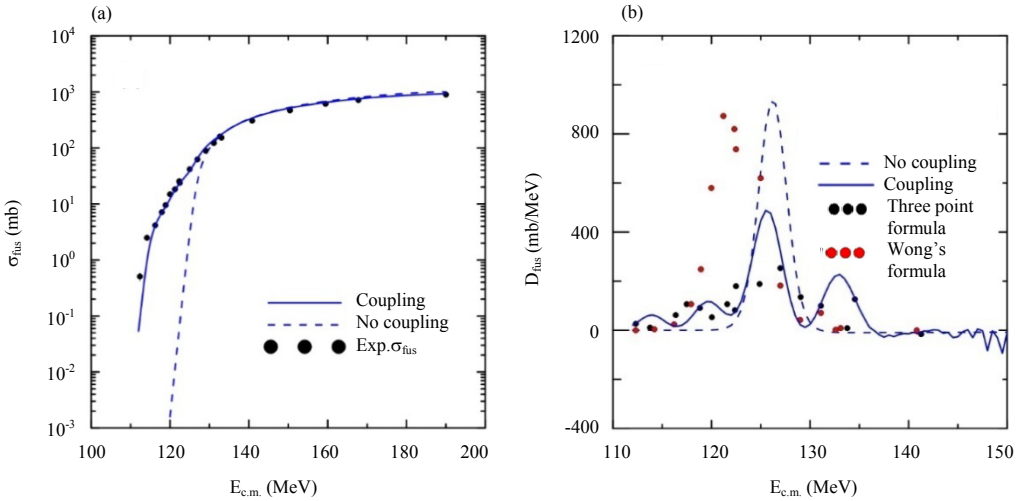

Fig. 3: (a) The experimental fusion cross section for $^{32}S+^{152}Sm$ along with results from CC calculations using CCFULL and (b) The fusion barrier distribution for the same system

that the coupling curve has a good approach with experimental data with a little bit difference in low energies. The Woods-Saxon parameters are displayed in Table 1 with fusion barrier height equals to 126.24 MeV and radius 10.43 fm.

Figure 3b shows the calculated fusion barrier distribution for coupling (solid line), no-coupling (dashed line), extracted fusion barrier distribution using point difference formula (black circle) and the calculated using Wong's formula (red circle) (Najim *et al*., 2019). We note that the coupling curve and extracted fusion barrier distribution using point difference formula showed almost four peaks for each one while the fusion barrier calculated by Wong's formula showed two peaks. The little oscillation of coupling curve above 145 MeV pointing out the needing to a deeper potential.

$^{32}S+^{154}Sm$ system: For this system, the coupling had been carried out for the rotational levels of ^{154}Sm nucleus along with vibrational modes of ^{32}S which are illustrated in Table 2 and 3.

Figure 4a shows the results of the calculated fusion cross section for $^{32}S+^{154}Sm$ system where the coupling curve (solid line), the no-coupling curve is represented by (dash line) and the experimental data (black circle) has been taken from reference (Glagola *et al*., 1984). The Woods-Saxon parameters are displayed in Table 1 they had been adjusted according to best possible value of the

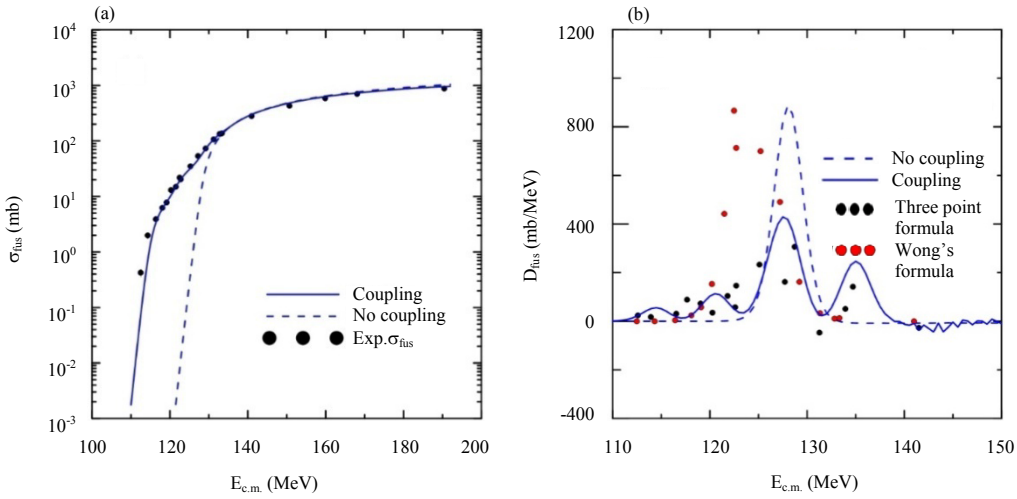

Fig. 4: (a) The experimental fusion cross section for $^{32}S+^{154}Sm$ along with results from CC calculations using CCFULL and (b) The fusion barrier distribution for the same system

diffuseness parameters a_0 which was 0.7 this set of parameters gives a fusion barrier height equals to 128.12 MeV and radius 10.35 fm.

Figure 4b shows the calculated fusion barrier distribution for coupling (solid line), no-coupling (dashed line), extracted fusion barrier distribution using point difference formula (black circle) and the calculated using Wong's formula (red circle) (Najim *et al*., 2019). It is noted that there is a convergent behavior of the coupling curve and the extracted fusion barrier distribution (black circle), due to the coupling to the excited collective states of collision partners. The fusion barrier distribution calculated by Wong's formula (red circle) showed only one peak. It is also noted that the little oscillation in calculated fusion barrier above energy 140 MeV due to the fact of shallow potential, means deeper potential should be taken but this will have effect on the calculations.

CONCLUSION

In all the systems under study, the coupling effects are very evident and distinguishable. The rotational coupling to the collective states of target nucleus in $^{32}S+^{152}Sm$ and $^{32}S+^{154}Sm$ systems agreed very well blow and above the Coulomb barrier with the corresponding data. Vibrational coupling was adopted for the calculations of $^{32}S+^{144}Sm$ and $^{32}S+^{150}Sm$ systems. Although, the coupling is considered for the systems $^{32}S+^{144}Sm$ and $^{32}S+^{150}Sm$ which enhances the calculations for the fusion cross section, it is still underestimated the experimental data below the Coulomb barrier. This short coming in describing the measured data might be attributed to the lack of including all coupling effects that might enhance the calculations but to include such coupling effects one need serious modification to the present approximated approach adopted by CCFULL. The disagreement between the calculate and extracted fusion barrier distribution, might be due to non-equal energy interval E for the extracted fusion barrier distribution due to the not equally spaced of experimental data while the Energy interval E which used in the calculated fusion barrier had been fixed at 2 MeV.

REFERENCES

Balantekin, A.B. and N. Takigawa, 1998. Quantum tunneling in nuclear fusion. Rev. Mod. Phys., 70: 1-55.

Canto, L.F. and R. Donangelo, 2009. Improved determination of the fusion barrier distribution. Phys. Rev. C., Vol. 79, 10.1103/physrevc.79.037601

Dasgupta, M., D.J. Hinde, N. Rowley and A.M. Stefanini, 1998. Measuring barriers to fusion. Annu. Rev. Nucl. Part. Sci., 48: 401-461.

Dasso, C.H., S. Landowne and A. Winther, 1983a. A study of Q-value effects on barrier penetration. Nucl. Phys. A., 407: 221-232.

Dasso, C.H., S. Landowne and A. Winther, 1983b. Channel-coupling effects in heavy-ion fusion reactions. Nucl. Phys. A., 405: 381-396.

Esbensen, H., 1981. Fusion and zero-point motions. Nucl. Phys. A., 352: 147-156.

Frobrich, P. and R. Lipperheide, 1996. Theory of Nuclear Reactions. Clarendon Press, Oxford, England, UK., ISBN: 9780198537830, Pages: 476.

Glagola, B.G., B.B. Back and R.R. Betts, 1984. Effects of large angular momenta on the fission properties of Pt isotopes. Phys. Rev. C., 29: 486-497.

Hagino, K. and N. Takigawa, 2012. Subbarrier fusion reactions and many-particle quantum tunneling. Prog. Theor. Phys., 128: 1061-1106.

Hagino, K., 2016. Investigating multichannel quantum tunneling in heavy-ion fusion reactions with Bayesian spectral deconvolution. Phys. Rev. C., Vol. 93, 10.1103/PhysRevC.93.061601

Hagino, K., N. Rowley and A.T. Kruppa, 1999. A program for coupled-channel calculations with all order couplings for heavy-ion fusion reactions. Comput. Phys. Commun., 123: 143-152.

Kibedi, T. and R.H. Spear, 2002. Reduced electric-octupole transition probabilities, $B(E3;0_{1+}\rightarrow 3_{1-})$-an update. At. Data Nucl. Data Tables, 80: 35-82.

Leigh, J.R., M. Dasgupta, D.J. Hinde, J.C. Mein and C.R. Morton *et al*., 1995. Barrier distributions from the fusion of oxygen ions with ^{144,148,154}Sm and ^{186}W. Phys. Rev. C., 52: 3151-3166.

Majeed, F.A., R.S. Hamodi and F.M. Hussian, 2017. Semiclassical coupled channels calculations in Heavy-ion fusion reaction. Adv. Stud. Theor. Phys., 11: 415-427.

Majeed, F.A., Y.A. Abdul-Hussien and F.M. Hussian, 2019. Fusion Reaction of Weakly Bound Nuclei. In: Nuclear Fusion: One Noble Goal and a Variety of Scientific and Technological Challenges, Girka, I. (Ed.). IntechOpen, London, UK., ISBN: 978-1-78985-787-0, pp: 186-186.

Nagarajan, M.A., A.B. Balantekin and N. Takigawa, 1986. Geometric interpretation of the adiabatic model for heavy-ion fusion. Phys. Rev. C., 34: 894-898.

Najim, A.J., F.A. Majeed and K.H. Al-Attiyah, 2019. Improved calculation of fusion barrier distribution. IOP. Conf. Ser. Mater. Sci. Eng., Vol. 571, 10.1088/1757-899X/571/1/012124

Pritychenko, B., M. Birch, B. Singh and M. Horoi, 2016. Tables of E2 transition probabilities from the first 2+ states in even-even nuclei. At. Data Nucl. Data Tables, 107: 1-139.

Raghavan, P., 1989. Table of nuclear moments. Atomic Data Nucl. Data Tables, 42: 189-291.

Rowley, N., G.R. Satchler and P.H. Stelson, 1991. On the distribution of barriers interpretation of Heavy-ion fusion. Phys. Lett. B., 254: 25-29.